Title	Femtosecond electron deflectometry for measuring transient fields generated by laser-accelerated fast electrons
Author(s)	Inoue, Shunsuke; Tokita, Shigeki; Otani, Kazuto; Hashida, Masaki; Sakabe, Shuji
Citation	Applied Physics Letters (2011), 99(3)
Issue Date	2011-07
URL	http://hdl.handle.net/2433/145988
Right	© 2011 American Institute of Physics
Type	Journal Article
Textversion	publisher

Femtosecond electron deflectometry for measuring transient fields generated by laser-accelerated fast electrons

Shunsuke Inoue,[1,2,a)] Shigeki Tokita,[1,2] Kazuto Otani,[1,2] Masaki Hashida,[1,2] and Shuji Sakabe[1,2]
[1]*Advanced Research Center for Beam Science, Institute for Chemical Research, Kyoto University, Gokasho, Uji, Kyoto 611-0011, Japan*
[2]*Department of Physics, Graduate School of Science, Kyoto University, Kitashirakawa, Sakyo, Kyoto 606-8502, Japan*

(Received 18 May 2011; accepted 27 June 2011; published online 22 July 2011)

The temporal evolution of the electric field generated near the surface of a solid target by a femtosecond laser pulse with intensity of 1×10^{16} W/cm^2 has been investigated by electron deflectometry; in this technique, ultrashort electron pulses generated by intense femtosecond laser pulses are used as probes. We found that electric field of the order of 10^8 V/m along the target surface was generated and decayed within 400 fs. The results of this study demonstrate the potential of electron deflectometry for measuring ultrafast phenomena in the femtosecond time domain. © *2011 American Institute of Physics*. [doi:10.1063/1.3612915]

The generation and transport of fast electrons via the interaction between an intense femtosecond laser pulse and solid target are fundamental processes that must be better understood in order to realize advanced applications, such as fast ignition for laser inertial confinement fusion,[1–4] target-normal sheath ion acceleration,[5–8] ultrashort electron pulse generation,[9,10] and high-quality X-ray production.[11] Recently, to study the dynamics of fast electrons, direct measurements have been performed by employing laser-accelerated proton beams to probe laser-induced electric fields.[12–16] These diagnostic techniques, namely, proton radiography and proton deflectometry, provide temporal resolution as high as a few picoseconds for measuring electric fields. The temporal resolution of these techniques, however, is insufficient for observing the electric field generated by fast electrons produced during and immediately after a laser pulse. The temporal resolution is determined by the pulse duration of the proton beam, which is limited to the order of picoseconds.[16] Electron pulses generated by an electron gun have also been used to measure ultrafast electric fields.[17–19] Hebeisen *et al.* measured electric field strength to be 3.5×10^6 V/m at 3 ps after laser excitation.[17] For further study of interactions between intense femtosecond laser pulses and matter, investigating electric field dynamics on a time scale of hundreds of femtoseconds has become necessary.

In this paper, we present the fast electron dynamics within several hundreds of femtoseconds after a solid target was irradiated with a laser pulse. The measurement object was produced by irradiating a solid target with an intense femtosecond laser pulse, and an electron beam probe was also generated next to the measurement object on the same target; in this manner, high temporal resolution was successfully realized.

The experimental setup is shown in Fig. 1. The laser beam from a chirped pulse amplification Ti:sapphire laser system[20] was split into upper and lower half-beams by means of a dual-partitioned gold mirror. The two beams were focused onto the target in proximity to each other with *p*-polarization at an incident angle of 45° by using an *F*/3 off-axis parabolic mirror. The upper and lower beams had the same focal spot size of 4×7 μm^2 (full width at half-maximum (FWHM)). Each gold mirror was set in an independent mirror holder, thus allowing the distance between the two focal positions for the upper and lower laser pulses to be adjusted. The distance between the two spots was varied between 30 μm and 240 μm. The mirror for the lower pulse was held on a motor stage in order to control the time delay between two pulses. The laser pulse duration was 200 fs FWHM, and the laser pulse energy was set such that the intensity of each pulse on the target was 1×10^{16} W/cm^2. The contrast ratio between the intensities of the main pulse and the amplified spontaneous emission (5-ns duration) was measured to be 10^{-7} by a third-order cross correlator. The target was aluminum foil of 12 μm in thickness and was installed on a rotating stage in order to provide a fresh surface for each pulse. The position of the target surface was carefully measured with a laser micrometer and adjusted so that the position displacement was less than ± 3 μm in the laser propagation direction. The two laser pulses produced two

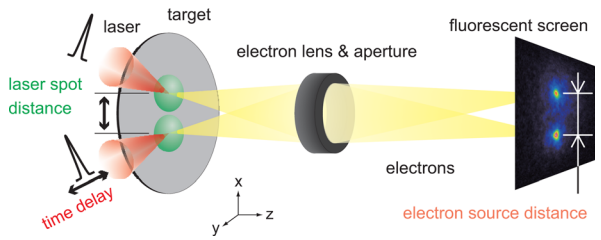

FIG. 1. (Color online) Schematic of the experimental setup. Two laser pulses with a time delay between them are focused on an Al target (thickness: 12 μm) to produce electron pulses. The distance between the focal points of the two laser pulses and the time delay between them are variable. The laser-produced electrons are emitted isotropically. Some part of the electrons emitted along the target-normal direction can be focused on a fluorescent screen by an electron lens. The electron pulses are deflected by each of the laser plasmas immediately after they are emitted from target; consequently, the source image position on the fluorescent screen is different from that when another laser plasma does not exist.

[a)]Author to whom correspondence should be addressed. Electronic mail: sinoue@laser.kuicr.kyoto-u.ac.jp.

adjacent pulsed electron sources. The angular distribution of electron emission was measured separately with an imaging plate and was almost uniform in space. As shown in Fig. 1, the electrons emitted in the target-normal (z-axis) direction could be collected, and the emission sources could be magnified and imaged with high spatial resolution by means of an electron imaging system that consisted of an electron lens and fluorescent screen.[21] The lens was set 17 mm behind the electron sources and had an aperture of 300 μm in diameter (solid angle 2.4×10^{-4} sr). The sensitivity of this electron imaging system is sufficiently high to obtain a distinct image in a single shot, and the energy of electrons imaged on the screen is selected by the lens; specifically, when the screen is placed 730 mm from the lens, the energy of imaged electrons is 120 keV.[21] The spectrum of electrons emitted along the z-axis was also separately measured with a magnetic spectrometer and could be fitted to the Boltzmann distribution with the temperature corresponding to ~40 keV.

The deflection of the electron pulses was determined from the distance between the two electron source images on the fluorescent screen. When there is no influence of electromagnetic field induced by laser-produced electrons, the distance on the screen corresponds to the physical distance between the two laser spots with the magnification ratio of the imaging system. When the time delay between the upper and lower laser pulses is small, each electron pulse will be deflected along the target surface by the electromagnetic force (mainly Coulomb repulsive force) from each laser-produced plasma, immediately after being emitted from the target; consequently, the positions imaged on the screen will be displaced from the original position. This amount of displacement essentially includes information on the electromagnetic field along the target surface. We measured the distance between the two electron source images on the screen while varying the time delay and the laser spot distance. Carefully adjusting the energy and the spot diameter of the upper laser pulse to be equal to those of the lower laser pulse, we can consider that each electron pulse serves as a pump pulse and a probe pulse, and we can calculate the autocorrelation of the electron pulses.

Figure 2(a) shows typical images obtained by a series of deflectometry measurements. Each of these images was obtained by a single laser shot. Figure 2(b) shows intensity distributions crossing the position of the maximum intensity for each of the two sources in Fig. 2(a). The distance between the two electron source images was determined from Fig. 2(b). In these images, the distance between two peaks of laser spots was 50 μm. When the time delay between two laser pulses was −2.1 ps or 2.1 ps, the distance between the two electron source images was equal to that between the two laser irradiated spots. When the time delay was −0.46, 0, or 0.46 ps, the distance of two electron images was less than 50 μm. These deflections were caused by the interaction between the two electron pulses emitted from the target surface. Immediately, as the two electron pulses were produced by the two laser pulses, the electron pulses were acted upon by Coulomb repulsion from each pulse and deflected. Since they were deflected close to the target and far enough away from the electron lens, the distance between electron source images on the screen becomes effectively shorter than the original distance. The repulsive force acts on the electron pulse as a concave lens. When the time delay was zero (two laser pulses irradiated at the same time), the deflection of the two electron pulses was maximum (distance between electron source images was minimum) as shown in Fig. 2.

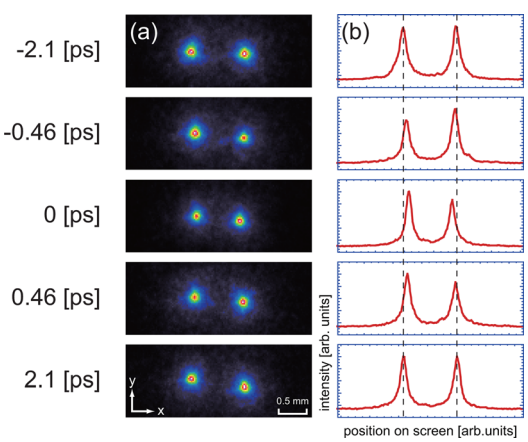

FIG. 2. (Color online) (a) Electron source images for time delays of −2.1, −0.46, 0, 0.46, and 2.1 ps and (b) one-dimensional intensity distributions crossing through each intensity peaks of (a).

Figure 3 shows the electron pulse deflections as a function of time delay for laser spot distances of 30, 50, 110, and 240 μm. At each time delay, the deflection was determined as the difference of the distance between the two electron images from that between the laser spots. The inset scale in Fig. 3 refers to the target plane. Each point was obtained by averaging the deflections obtained from 30-50 laser shots. The dispersion, measured as the standard deviation, was ± 2 μm. The solid lines in Fig. 3 are fitted to exponential functions to estimate the interaction time of the two electron pulses. As shown in Fig. 3, it was distinctly observed that the electron pulses were deflected by laser plasmas from −1 ps to 1 ps for the laser spot distance of 30 μm and that the interaction time was 400 ± 50 fs (temporal interval given by half width of e^{-1} maximum). If the electric field were perfectly shielded in the plasma, the electron pulses would not be deflected. Our results indicate that the electron pulses were deflected by the

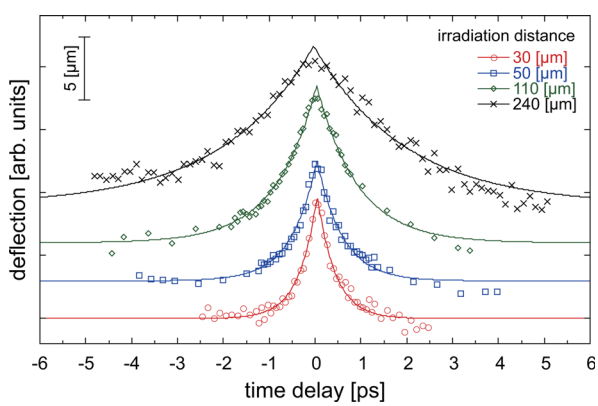

FIG. 3. (Color online) Electron pulse deflections as a function of time delay for laser spot distance of 30 μm (circle), 50 μm (square), 110 μm (diamond), and 240 μm (cross). The deflection is determined by the difference of the distance between the two electron source images from that between the laser spots. Each point is obtained by averaging the distances obtained from 30-50 laser shots. The solid lines are fitted to exponential functions to estimate the interaction times of the two electron pulses.

Coulomb repulsive force from each electron source immediately after electrons were emitted. As the distance between the laser-irradiated positions was increased, the interaction time became longer. The electric field generated by the electrons emitted toward the vacuum exists within several picoseconds and several hundreds of micrometers. After electron pulses are emitted, the electric field promptly decays to become no longer detectable. This means that the electron pulses are emitted far from the target, and consequently that the electric field along the target surface becomes zero. If the electron pulses were deflected by the residual charge (positive charge) at the laser spots on the target, the deflection direction would be reversed so that the distance between the electron source images on the screen would be longer than that between the laser spots. In our experiments, such reversed deflection was not observed, and thus, only the electric field induced by the electron pulses influences their deflection.

For discussion, a schematic of electron deflection by the Lorentz force around the target surface and the trajectory through the lens to the screen are shown in Fig. 4. The electrons are emitted almost isotropically, and then the electrons passing through the lens are focused on the screen. The solid lines indicate electron rays including the principal rays through the electron lens, for the simultaneous irradiation of the two laser pulses. Two electron pulses are generated and deflected by the Lorentz force. The distance between two electron source images on the screen becomes shorter. Assuming that the temporal variation of electric field does not depend on the time delay between the two electron pulses, we can calculate this electron deflection as a function of time delay. Since the principal ray is almost parallel to the optical axis in the experimental setup, the electron pulse deflection $d(\tau)$ as a function of time delay τ is given by

$$d(\tau) = -\frac{e}{m_e\gamma}\int\int_{\tau} dt^2[E_x(t) + c\beta B_y(t)], \qquad (1)$$

where $E_x(t)$ is the electric field along the x direction and $B_y(t)$ is the magnetic field along the y direction (axes shown in Fig. 1), e is the elementary charge, and m_e is the electron mass. The kinetic energy of electron pulses observed here is 120 keV, and thus, we take account of relativistic effects: γ is

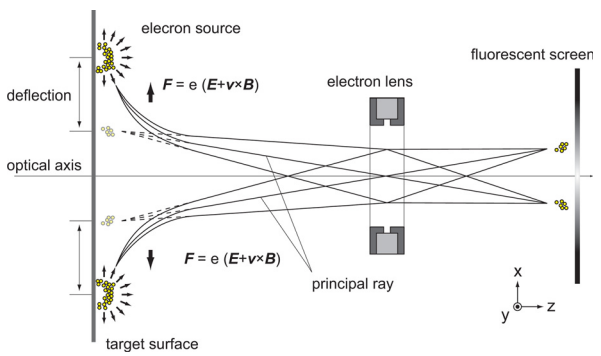

FIG. 4. (Color online) Schematic for the trajectories of the electrons measured with the imaging system. Solid lines show trajectories of the electron pulses deflected by electromagnetic field. The electron pulses are observed as if they were generated from the position indicated by the dashed lines.

the Lorentz factor and β is the ratio of electron velocity to the speed of light. The observed electron velocity is not so high ($\beta = 0.59$) that the second term on the right-hand side of Eq. (1) can be restrictive. Furthermore, since the electrons are emitted isotropically, the effect of the magnetic field produced by electron pulse current is small. Here, we can neglect the second term of Eq. (1). From Fig. 3, we can assume that $d(\tau)$ decays exponentially. Accordingly, Eq. (1) can be reduced to

$$d(\tau) = -\frac{\alpha^2 eE_0}{m_e\gamma}\exp\left(-\frac{\tau}{\alpha}\right),$$

where E_0 is the maximum of electric field at $\tau = 0$ and α is the decay time. By substituting $\alpha = 400$ fs and $d(\tau = 0) = 4.9$ μm from the experimental result where the distance between laser spots was 30 μm, the magnitude of the electric field when the beam deflects to the maximum is estimated to be $\sim 2 \times 10^8$ V/m.

In summary, we have demonstrated femtosecond electron deflectometry employing femtosecond laser-accelerated electron pulses and a high-spatial-resolution electron imaging system. We observed the deflection of electron pulses during a period of several hundreds of femtoseconds after the laser pulse was irradiated on a solid target. The observed deflections were qualitatively explained by the transient electric fields produced by electron pulses. These results indicate that the electric field along the target surface decayed in 400 ± 50 fs or less and that the magnitude of the electric field was $\sim 2 \times 10^8$ V/m, when the laser spots were separated by 30 μm for laser intensity of 1×10^{16} W/cm^2. This study shows that electron deflectometry using laser-accelerated electron pulses is a promising diagnostic technique for ultrafast electric field measurements.

This work was supported by KAKENHI (18206006, 22654050, and 22760038) and the Global COE Program "The Next Generation of Physics, Spun from Universality and Emergence" from the Ministry of Education, Culture, Sports, Science and Technology (MEXT) of Japan.

[1]M. Tabak *et al.*, Phys. Plasmas **1**, 1626 (1994).
[2]S. Atzeni, Phys. Plasmas **6**, 3316 (1999).
[3]Y. T. Li *et al.*, Phys. Rev. Lett. **96**, 165003 (2006).
[4]R. Kodama *et al.*, Nature **412**, 798 (2001).
[5]S. C. Wilks *et al.*, Phys. Plasmas **8**, 542 (2001).
[6]M. Roth *et al.*, Phys. Rev. ST Accel. Beams **5**, 061301 (2002).
[7]P. McKenna *et al.*, Phys. Rev. Lett. **98**, 145001 (2007).
[8]S. Buffechoux *et al.*, Phys. Rev. Lett. **105**, 015005 (2010).
[9]S. Tokita *et al.*, Appl. Phys. Lett. **95**, 111911 (2009).
[10]S. Tokita *et al.*, Phys. Rev. Lett. **105**, 215004 (2010).
[11]Ch. Reich *et al.*, Phys. Rev. Lett. **84**, 4846 (2000).
[12]M. Borghesi *et al.*, Phys. Plasmas **9**, 2214 (2002).
[13]L. Romagnani *et al.*, Phys. Rev. Lett. **95**, 195001 (2005).
[14]T. Sokollik *et al.*, Appl. Phys. Lett. **92**, 91503 (2008).
[15]K. Quinn *et al.*, Phys. Rev. Lett. **102**, 194801 (2009).
[16]G. Sarri *et al.*, New J. Phys. **12**, 045006 (2010).
[17]C. T. Hebeisen *et al.*, Phys. Rev. B **78**, 081403(R) (2008).
[18]M. Centurion *et al.*, Nature Photon. **2**, 315 (2008).
[19]J. Li *et al.*, Appl. Phys. Lett. **98**, 011501 (2011).
[20]S. Tokita *et al.*, Opt. Express **16**, 14875 (2008).
[21]S. Inoue *et al.*, Rev. Sci. Instrum. **81**, 123302 (2010).
[22]General Particle Tracer, http://www.pulsar.nl/gpt